CHEMISTRY
AN ASIAN JOURNAL
www.chemasianj.org

Accepted Article

Title: A hemicyanine-embedded diphenylselenide-containing probe "HemiSe" in which SePh2 stays reduced for selective detection of superoxide in living cells

Authors: Mahesh B. Halle, Kyung Jin Lee, Tesla Yudhistira, Jae Hyuck Choi, Hee-Sung Park, and David G. Churchill

To be cited as: *Chem. Asian J.* 10.1002/asia.201801339

Link to VoR: http://dx.doi.org/10.1002/asia.201801339

A Journal of
ACES Asian Chemical Editorial Society

A sister journal of Angewandte Chemie and Chemistry – A European Journal

WILEY-VCH

10.1002/asia.201801339

WILEY-VCH

FULL PAPER

A hemicyanine-embedded diphenylselenide-containing probe "HemiSe" in which $SePh_2$ stays reduced for selective detection of superoxide in living cells

Mahesh B.Halle,[a]+ Kyung Jin Lee,[d]+ Tesla Yudhistira,[a]+Jae Hyuck Choi,[a] Hee-Sung Park,[d] and David G. Churchill*[a],[b],[c]

Dedication ((optional))

Abstract: A simple one-step synthesis of fluorescent probe **HemiSe** has been developed for the detection of superoxide ($O_2^{\bullet-}$). The probe undergoes reaction specifically with $O_2^{\bullet-}$ when in the presence of other competitive ROS/RNS/metal ions. The diphenylselenide was incorporated to completely quench the fluorescence of the hemicyanine unit through the action of a photoinduced electron transfer (PET) photomechanism. However, after the addition of $O_2^{\bullet-}$, the latent fluorophore regains its fluorescence due to the reaction at the C=C bond of the hemicyanine with $O_2^{\bullet-}$ through nucleophilic attack; the increase in blue emission is due to a reaction of the double bond within **HemiSe** followed by an increase in fluorescence quantum yield (Φ) up to 0.45; the limit of detection (LOD) is 11.9 nM. A time dependent study shows that **HemiSe** can detect superoxide within 13 min with high sensitivity, high selectivity, over a wide pH range, and through confirmation with a xanthine/xanthine oxidase biochemical assay (λ_{em} = 439 nm). Study in the RAW 264.7 macrophage living cells also shows that **HemiSe** is not toxic, cell permeable (experimental log P = 2.11); confocal imaging results show that HemiSe can detect $O_2^{\bullet-}$ in endogenous and exogeneous systems.

Introduction

Reactive oxygen/nitrogen species (RO/NS) such as H_2O_2, HOCl, •OH, $O_2^{\bullet-}$, NO, ONOO−, ^{t}BuOOH, and ^{t}BuOO• are oxygen/nitrogen-containing species synthesized inside cells in low concentration.[1] These species are well known for their role in killing microbial cells or pathogens as a part of the cells' defense system.[2] Recent biological studies have revealed that ROS are capable of regulating normal biological and physiological functions as well. For example, low concentrations of ROS can activate the signaling pathways and trigger important biological processes such as cellular proliferation and differentiation.[3] However, intracellular oxidative stress that relate to an imbalance in concentration between ROS and cellular antioxidant (such as glutathione) concentration affect DNA, proteins and lipids. The eventual oxidation of the biomolecules results in cell death, cell proliferation, and also inflammation within the central nervous system (CNS); these effects are also definitely seen in, or possibly linked to the etiology of neurodegenerative disorders as well as primary and metastatic brain tumors.[4]

Superoxide radical anion ($O_2^{\bullet-}$) is the major reactive oxygen species (ROS) in living systems.[5] This species is involved in signaling transduction and serves as a precursor for other ROS such as hydrogen peroxide (H_2O_2), hydroxyl radical (•OH), singlet oxygen ($^1O_2$) and hypochlorous acid (HOCl) by the disproportionation of H_2O_2 and $O_2^{\bullet-}$.[6] The excessive amounts of $O_2^{\bullet-}$ could lead to oxidative damage of a variety of essential biomolecules such as various proteins, DNA, or array lead to cell apoptosis.[7] These ROS/RNS species are associated with signal transduction and diverse pathological conditions, including Alzheimer's disease, amyotrophic lateral sclerosis, Parkinson's disease,[8] cardiomyopathy,[9] atherosclerosis,[10] rheumatoid arthritis,[11] diabetes mellitus,[12] pulmonary arterial hypertension,[13] and also ischemia[14]. Therefore, it is very important to develop useful methods that address high sensitivity and good selectivity for the detection of e.g. , $O_2^{\bullet-}$ in living biological samples. Luckily, the vast differences in chemical properties of various ROS, such as half-life, reactivity, and cellular compartmental distribution, make specific detection of single ROS in live cells possible. [15,16]

To date, there are a wide array of analytical methods and approaches which have been developed for the detection of $O_2^{\bullet-}$. The methods include mass spectrometry (MS),[17] colorimetric,[18] electrochemical analysis,[19] high performance liquid chromatography (HPLC),[20] and electron paramagnetic resonance spectroscopy (EPR).[21] However, these methods are hindered by certain disadvantages. In some cases, extracellular detection, time consuming experimentation, expensive apparatus

[a] Dr. M. B. Halle, T. Yudhistira, J.H. Choi, Prof. Dr. D. G. Churchill
Molecular Logic Gate Laboratory, Department of Chemistry, Korea Advanced Institute of Science and Technology (KAIST), Daejeon, 305–701, Republic of Korea. E-mail: dchurchill@kaist.ac.kr.
[b] Prof. Dr. D. G. Churchill
Center for Catalytic Hydrocarbon Functionalizations, Institute for Basic Science (IBS), Daejeon, 305−701, Republic of Korea.
[c] Prof. Dr. D. G. Churchill
KI for Health Science and Technology, KI Institute, Korea Advanced Institute of Science and Technology (KAIST), Daejeon, 305-701, Republic of Korea
[d] K. Lee, Prof. Dr. H.-S. Park
Department of Chemistry, Korea Advanced Institute of Science and Technology (KAIST), Daejeon, 305–701, Republic of Korea.
+ These authors have equal contribution in this work.

Supporting information for this article is given via a link at the end of the document.((Please delete this text if not appropriate))

10.1002/asia.201801339

and methodology, and the requirements of utilizing experienced personnel to obtain valid data all represent potential limitations or bottle necks in achieving perfection when considering the current best practices. On the other hand, organic fluorescent probes have become more and more reliable for monitoring bioactive molecules and have transformed from a corpus of sporadic reports to an important and large methodologic biological field of study that interfaces with a multitude of other criteria; it bears major advantages such as good selectivity, high sensitivity, and real-time detection.[22] Thus, the design and development of small molecule fluorescent probes for the detection of analytes such as $O_2^{\bullet-}$ under physiological conditions have attracted the interest and efforts of many scientists around the globe because of the non-invasiveness, fast response, highly sensitive, and simplicity of the detection media.[23]

In recent years, many scientific research groups have been developing fluorescent probes embedded with specific functional groups such as diselenide (e.g. by the Churchill group),[24] cyclohexene dibenzothiazoline (e.g. by the An group),[25] hydroethidine[26] and boronate (e.g. by the Kalyanaraman group),[27] and also phosphinate (by the Zhang group)[28] which all possess specific capabilities or capacity to detect $O_2^{\bullet-}$. However, only a few examples among these can be used for "real-time" detection in biological investigations. Limitations include low selectivity, sensitivity, poor photostability and/or chemostability and high probe molecular weight.[29]

Organochalcogenide (S, Se, and Te)-containing systems are extensively utilized in various fields of biomedical research. Our research group has been engaged in synthesizing several fluorescent systems containing chalcogenide (S, Se, and Te) functionalities as an exploration of ROS/RNS reactive moieties within chemosensing.[30] These reactive moieties (involving an electron rich Se center) are incorporated within the fluorophore and act as modulators to the fluorescence intensity for systems which are inherently fluorescent; based on redox action, the reactivity of the Se can be related to the inherent reactivity and concentration of ROS/RNS species and their concentration in biological systems. It is well known that the diphenylselenide moiety has an ability to undergo reaction with ROS/RNS rapidly. Hence, it can be used as a real-time chemosensor for the detection of ROS/RNS.[31]

In addition, our group has developed and synthesized a selective and sensitive superoxide anion radical fluorescent probe based on the diselenide - BODIPY systems. [24] Based on that concept, we have designed a new probe presented herein. It is novel, important and simple to prepare. Hemicyanine is a well-known fluorescence molecule which is widely used due to its shift in molecular charge upon electron excitation. This property is useful in detecting the variations in the membrane potentials of biological materials.[32] Herein, we incorporated a hemicyanine derivative with a diphenylselenide substituent **(HemiSe**) for monitoring the superoxide radical anion in which there are two possible available ROS reaction sites. In this system, the diphenylselenide modulates the fluorescence of the hemicyanine by quenching the fluorescence before the reaction with superoxide through a photoinduced electron transfer (PET) mechanism. However, after the reaction with superoxide radical anion, the fluorescence of **HemiSe** is restored due to the reaction between the superoxide and the styryl like double bond between the diphenylselenide and hemicyanine which is proposed to accept a peroxide group, thus, cancelling the PET effect. The observed "turn-on" fluorescence reaction towards superoxide when in the presence of other ROS/RNS and metal ions is important. The blue signal is similar to a previous reported hemicyanine system. [33]

Further study with RAW 264.7 macrophage cells suggests that the probe is reliable as a chemosensor to image the concentration level of superoxide radical anion exogenous and endogenous in living cells.

Results and Discussion

The synthesis of **HemiSe** is presented in Scheme 1. The 2-(phenylseleno)-benzaldehyde starting material, was synthesized according to a known literature route;[37] then, the intermediate was subsequently allowed to undergo reaction with 1H-benz[e]indolium,1,1,2,3-tetramethyl-hexafluorophosphate through a simple condensation reaction to allow for **HemiSe** to be obtained in good yield (56%) out of toluene solvent as a non-fluorescent species. The nature and structure of the **HemiSe** probed and characterized by spectroscopic techniques (multinuclear NMR spectral data, mass spectroscopy, FT-IR, and DFT calculations, Figures S1–S16, Supporting Information)

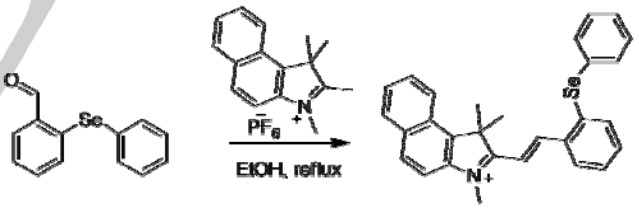

Scheme 1. Synthesis of **HemiSe**

The UV-vis absorption characteristics of **HemiSe** showed two typical bands centered at 425 nm and 359 nm. Then, after the addition of 3.0 equiv. of $O_2^{\bullet-}$, the absorption peak at 425 nm disappeared; a shoulder positioned at 360 nm then appeared. This new peak suggested that, after the reaction with $O_2^{\bullet-}$, a blue shift in the absorption peak occurs (from 425 nm to 360 nm) (Figure 1). In addition, **HemiSe** probes were also treated with other ROS/RNS; however, no changes in the UV-vis spectrum were observed toward other ROS/RNS (Fig S7-S8, Supporting Information).

10.1002/asia.201801339

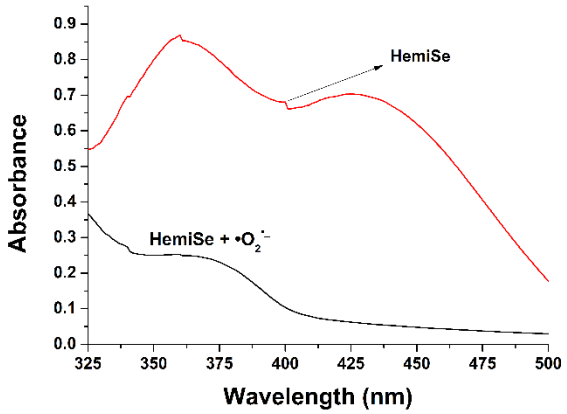

Figure 1. UV-vis Absorption spectra of **HemiSe** (20 μM) (red) and **HemiSe** (20 μM) with addition of 3.0 equiv. of $O_2^{\bullet-}$ (black) in the solution of PBS buffer (10 mM, pH 7.4): DMF: 7:3 (v/v); incubated for 15 min.

The selectivity of **HemiSe** with other ROS/RNS was investigated with spectrofluorometry. Before the addition of $O_2^{\bullet-}$ the fluorescence intensity of **HemiSe** was very weak (Φ_f = 0.023). We did not observe any significant changes in the fluorescence intensity after the addition of H_2O_2, HOCl, •OH, NO, $ONOO^-$, ^tBuOOH, $^1O_2$, Vc, HQ, Cys, GSH and $^tBuOO\bullet$ (Figures 2 and S16, Supporting Information). However, after the addition of 3 equiv of $O_2^{\bullet-}$ the blue emission centered at ($\lambda_{em,max}$) 439 nm increased 20-fold. The fluorescence quantum yield (Φ) of the **HemiSe** was from 0.023, related to the intramolecular photoinduced electron transfer (PET) due to the incorporation of the diphenylselenide. In addition, we also tested **HemiSe** with anion with nucleophilicty such as CN^-, SO_3^{2-}, and HSO_3. Our result revealed that **HemiSe** also give slightly "turn-on" fluorescence with the addition of SO_3^{2-}, and HSO_3, but not to CN^-. We also observed that the emission after the addition of (5 equiv) SO_3^{2-}, and HSO_3 is faint compared to the addition of (5 equiv) $O_2^{\bullet-}$ to HemiSe (Fig S17, Supporting Information).[36] Furthermore, addition of $O_2^{\bullet-}$, give a significant increase in the fluorescence quantum yield (Φ_f) up to a value of Φ_f = 0.45. This phenomenon appears to be due to an intermediate formulated as a hydroperoxide compound within hemicyanine framework (**HemiSe[OOH]**) (Figure 4).

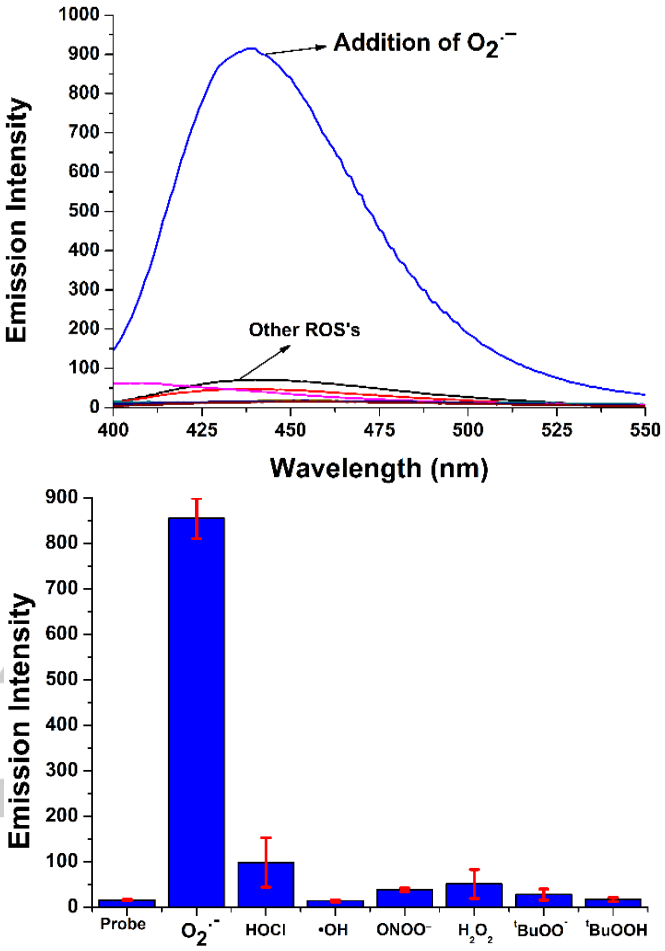

Figure 2. (Top) Selectivity study of **HemiSe** (10 μM) with $O_2^{\bullet-}$ (3 equiv.) and other reactive oxygen/nitrogen species (RO/RNS) such as H_2O_2, HOCl, •OH, $ONOO^-$, ^tBuOOH, and $^tBuOO\bullet^-$ (10 equiv) in the presence of PBS (pH 7.4): DMF: 7:3 (v/v); incubated for 15 min; λ_{ex}= 360 nm and λ_{em} = 439 nm; slit width (5 nm/ 5 nm). (Bottom). Bar graphs representative of the titration study performed (Experiments were performed 3 times). No reversibility was found when biothiols (L-cysteine, homocysteine, and glutathione) was added.

Titration of **HemiSe** with various concentration of $O_2^{\bullet-}$ was carried out. The experiment supported that the fluorescence intensity of **HemiSe** was gradually increased upon the addition of $O_2^{\bullet-}$ from 0 to 15.0 equiv; linearly proportional behavior was found through this addition of $O_2^{\bullet-}$ (Fig. S9, Supporting Information). **HemiSe** reached a saturation signaled by a maximum intensity of 14.0 equiv of $O_2^{\bullet-}$ added in the context of 15 min incubation time. Further investigation helped determine the detection limit of the **HemiSe** probe ($3\sigma/k$, where σ stands for the standard deviation of 10 blank samples measurements; k is the slope of the line produced from the equation generated by straight plot line fitting of the data); thus, the limit of detection was determined to be 11.9 nM (Fig. S10, Supporting Information).

10.1002/asia.201801339

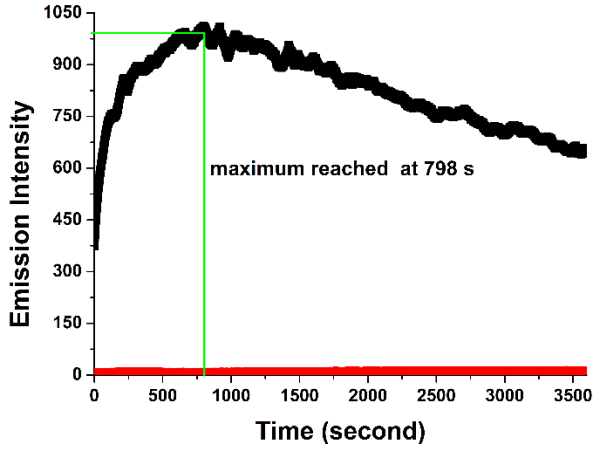

Figure 3. Time dependent experiment of **HemiSe** (10 μM) with 3.0 equiv. of $O_2^{\bullet-}$ in solution containing PBS (10 mM, pH 7.4): DMF: 7:3 (v/v); incubated for 3600 seconds; λ_{ex}= 360 nm and λ_{em} = 439 nm; slit width (5 nm/ 5 nm).

Next, an interference study of $O_2^{\bullet-}$ with other ROS/RNS and metal ions was performed. The results showed that other ROS/RNS did not give any change in the emission spectrum of the **HemiSe** (Fig. S11, Supporting Information). Furthermore, the presence of metal ions such as Ca^{2+}, Co^{2+}, Fe^{3+}, Fe^{2+}, Hg^{2+}, Li^{+}, Mg^{2+}, Mn^{2+}, Na^{+}, Pb^{2+}, Zn^{2+}, and K^{+} in PBS solution (10 mM, pH 7.4: DMF: 7/3 (V/V)) separately with both **HemiSe** and $O_2^{\bullet-}$ also did not alter the emission intensity of **HemiSe** (Fig. S.12, Supporting Information). These results suggested that metal ions and ROS/RNS did not interfere in the apparent reaction between **HemiSe** and $O_2^{\bullet-}$ or bind in a resulting complex.

To observe the kinetics of the reaction between **HemiSe** and $O_2^{\bullet-}$, we employed time-dependent experiments. The addition of 3.0 equiv. of $O_2^{\bullet-}$ into **HemiSe** showed "turn-on" fluorescence; within 13 minutes, the emission reached a maximum intensity (Figure 3). In accordance to the fluorescence of the **HemiSe**, we observed a slight decrease in the emission intensity after 15 min; however, the decrease in the emission intensity was not significant; after 60 min, the blue emission of the **HemiSe** still persisted. This result suggested that the reaction between **HemiSe** and $O_2^{\bullet-}$ was relatively fast and useful for real-time imaging of $O_2^{\bullet-}$ in living cells.

In order for it to be used reliably as a chemosensor in living cells, the **HemiSe** should be stable over a wide pH range. Thus, the fluorescence intensity of the **HemiSe** was measured throughout a wide range of pH values (Fig. S13, Supporting Information). These pH studies showed that the pH does not affect the emission of the **HemiSe**, especially in the neutral and basic region. The addition of 3.0 equiv of $O_2^{\bullet-}$ to **HemiSe** resulted in a strong emission within the pH 7 to pH 10 regime; under acidic conditions the emission intensity of the probe decreased significantly. These results suggest that **HemiSe** is stable and can be properly used considering the physiological conditions of the human body and other biological systems.

We contend that dye aggregation is not at play because measurements were performed at substantially low concentration (10^{-5} M). Based on the presence of the reduced selenium and the change in the fluorescence and optical properties at low concentration, we propose a chemical change to the probe that relates to chemistry seen with unsaturated fatty acids. Hydroperoxide formation in unsaturated lipids is known to produce a hydroperoxide intermediate. Ultimate reaction products might be carbonyl-containing fragments.

Molecular frameworks from the Scifinder Scholar database system shed some light on oxygen species of this type. At the styryl C=C, O is attached to the carbon bond moiety in a few cases. When we searched the literature, we found closely related examples that necessarily include the naphthyl framework: (2-(3-methyl-1,3-dihydro-1,1-dimethyl-2H-benz[e]indol-2-ylidene)-1-[4-phenyl]-ethanone) bearing the 5 membered indole group; other related molecules are also known; in some cases, fluorescence characteristics of the target molecules are reported. Attack at the carbon position in the double bond distal to the indole group results in our proposed structure for **HemiSe[OOH]**. The only known species at all similar to the intermediate are the ones that bear a carbonyl group at the benzylic position; thus, we propose the attachment of the hydroperoxyl group at this carbon (Fig. S25A, Supporting Information).[33,34] Regarding oxygenation at the 5-membered ring next to the nitrogen, there are some spiro examples from different previous research efforts that give insights on what might be available to the framework when considering the presence of benzene group positioning, namely the connecting phenylene of the Ph_2Se group. Somewhat related molecules are also known, albeit the spiro type, (Fig. S25B, Supporting Information): 1,3-dihydro-1,1,3-trimethyl-spiro[2H-benz[e]indole-2,2'-[2H-1]benzopyran]-8'-yl)methyl ester (or the 1',3'-dihydro-1',1',3'-trimethyl-spiro[2H-1-benzopyran-2,2'[2H]benz[e]indole]). The formulated **HemiSe[OOH]** therefore may undergo further chemistry which may bear a strong solvent dependence. Whether the selenium partakes of reactivity or binding in the proposed **HemiSe[OOH] i**ntermediate is not known at present; but it may be possible and the important takeaway is the apparent ROS-based regiochemistry at play.[35]

In this study, it is well known that, in an analogous way, ROS are capable of oxidizing the molecule at the selenium to form selenoxide, However, in this study, we observed that due to signature changes in the UV-vis, fluorescence, as well as the ^{1}H-NMR, spectroscopic data, $O_2^{\bullet-}$ appears to attack tentatively the double bond between diphenylselenide and hemicyanine which forms the hydroperoxyl compound moiety. To help confirm the sensing mechanism of $O_2^{\bullet-}$ based on this hypothesis, the characterization of the oxidized species was carried out by HRMS data of the **HemiSe** with $O_2^{\bullet-}$ (3 equiv). The m/z peak at 524.0737 [M+Na^+] (found) is consistent with the formulation such as the formation of the peroxide moiety within the **HemiSe**. We proposed the formation of resonance following species: **HemiSe[OOH]** 523.1031 (calc.) [M+Na^+]; also 540.0844 [M+K^+] (found) can be compared with 540.0799 [M+K^+] (calc.) (Fig. S6, Supporting

10.1002/asia.201801339

Information). Accordingly, the formation of the dioxygen blocks intramolecular electron transfer from the diphenyl diselenide donor moiety to the hemicyanine moiety which results in the blockage of the proposed PET process and undergoes reaction to increase the emission intensity of **HemiSe**. This HRMS data support that hydroperoxyl formation occurs after the addition of $O_2^{\bullet-}$ to the **HemiSe** solution (Figure 4A). As a complement to the ^{1}H-NMR spectroscpic data, we also acquired the ^{77}Se NMR spectrum of **HemiSe** *before* and *after* the reaction with $O_2^{\bullet-}$ and compared the peak shift due to the reaction and proposed addition of $O_2^{\bullet-}$. An extremely modest shift of ^{77}Se NMR peak of **HemiSe** from 366.5 ppm (before the addition of $O_2^{\bullet-}$) to 372.8 ppm (after the addition of $O_2^{\bullet-}$) is observed. This small change is not thought to be the direct chemical oxidation of selenide to selenoxide; this would, in fact, result in a much higher value NMR spectral shift value (~800 ppm). To give more insight of the mechanism, we also compared ^{1}H-NMR data of **HemiSe** and **HemiSe[OOH]**. Addition of $O_2^{\bullet-}$to **HemiSe** shift ^{1}H-NMR peaks found at low field (8.0-8.5 ppm) to more upfield position (7.0-5.5 ppm). These shifts relates to the addition reaction at the double bond within **Hemise** with $O_2^{\bullet-}$. Even though the ^{1}H-NMR data is not clear, but ^{77}Se-NMR and HRMS data give idea about the double bond addition mechanism. In addition, the "turn-on" responses observed by SO_3^{2-} and HSO_3^- also confirm the addition of $O_2^{\bullet-}$ to the double bond (Fig S.17, Supporting Information).[36] The double bond present within cyanine with $O_2^{\bullet-}$ to form hydroperoxide-like compound (Figure 4B and Fig S18, Supporting Information). These points of evidence are also supported by previous reports by the results from the Wang and Das research groups which used hemicyanine derivatives with similar reaction mechanism towards nucleophilic analyte. After comparing our result and previous reported results; we determined that the blue signal emission spectrum of **HemiSe** and previous report are relatively similar (430-440) ppm. [36]

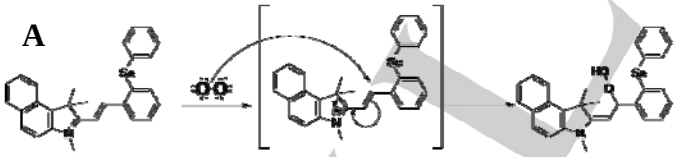

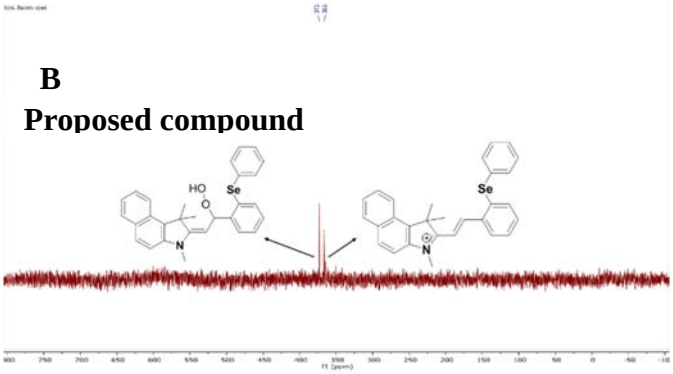

Figure 4. A) Proposed mechanism of **HemiSe** with superoxide anion radical anion; B) Comparison of ^{77}Se-NMR spectrum of HemiSe before (right peak) and after (left peak) the addition of $O_2^{\bullet-}$ in CD_3OD solution.

To help confirm the photomechanism and to gain more information about the reaction with ROS at play, density functional theory (DFT) and time-dependent DFT (TD-DFT) calculations were performed. Optimized structures were estimated by DFT calculations using the Gaussian 09 program. The B3LYP functional with a 6-31g* basis set was used and the 6-311g* basis set was used only for Se. The optimized structure of **HemiSe** and **HemiSe[OOH]** show that the phenylselenium undergoes rotation after the reaction in this model system. Before the reaction, the phenylselenium moiety is rearranged to be near the dimethyl position; however, the reaction with $O_2^{\bullet-}$ phenylselenium is located distal to the N-Me position. We proposed that this molecule undergoes nucleophilic attack and oxidizes at the double bond as shown; electron distribution spread around the nitrogen position of the cyanine system in which the distance between HOMO and LUMO energy level of **Hemise[OOH]** would be widened. The largest intense transition of **HemiSe** from HOMO-1 to LUMO (configuration interaction (CI) = 97.0 %), including an oscillator strength (f) of 0.2322, is defined as the dominant transition. In the case of **HemiSe[OOH]**, the oxidized system of **HemiSe**, the largest intense transition was found to exist from HOMO to LUMO+1 (CI = 96.7 %) with an oscillator strength of f = 0.1061 and a second intense transition goes from HOMO to LUMO+2 (CI =72.6 %) with an oscillator strength of F = 0.0891 (Fig. S23-S24, Supporting Information).

Furthermore, based on the DFT calculation data, the electronic distribution of the HOMO-1 of **HemiSe** is distributed within the molecule; whereas, the LUMO of the **HemiSe** is exhibited on the double bond and benzyl moiety of the diphenyl selenide group and provides a photoinduced electron transfer (PET) mechanism within the core of **HemiSe** ("turn-off" fluorescence). On the other hand, the HOMO and LUMO levels of **HemiSe[OOH]** electronic distributions overlap within the fluorophore core corresponding to fluorescence enhancement. This overlap can assist in explaining the "turn-on" fluorescence event found for the proposed **HemiSe[OOH]** spectrum. Moreover, the difference between the HOMO-1 and LUMO level for **HemiSe** is 2.79 eV; the difference between the HOMO-2 and LUMO of **HemiSe[OOH]** is 3.76 eV. According to the DFT calculations,

10.1002/asia.201801339

fluorescence enhancement arises from blocking the PET process and creating the expected blue-shift through the reaction of the isolated double bond within the molecule.

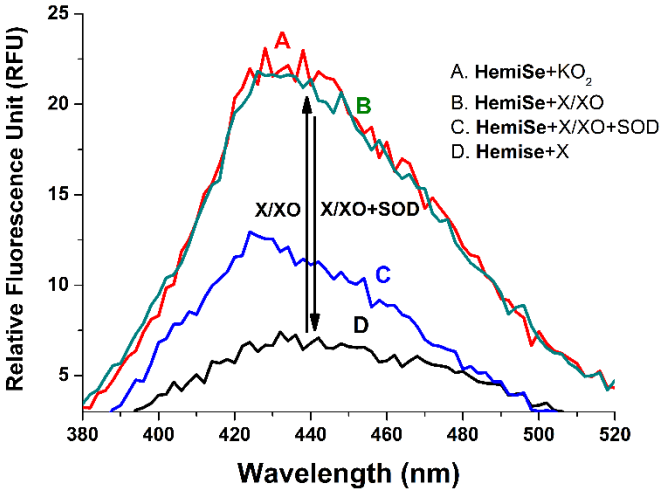

Figure 5. Effect of xanthine oxidase and SOD on the fluorescence intensity of the system of **HemiSe** with superoxide: A) **HemiSe** + KO_2 (final 100 μM), B) **HemiSe** + X/XO (final 2 mM/2 mU), C) **HemiSe** +X/XO + SOD (300 U); D) **HemiSe** (20 μM) + Xanthine (2 mM); added in PBS (50 mM, pH 7.4): DMF: 7:3 (v/v), incubated for 15 min; λ_{ex}= 360 nm and λ_{em} = 439 nm; slit width (5 nm/ 5 nm); X = xanthine; XO = xanthine oxidase.

To further confirm the selectivity of **HemiSe** towards $O_2^{\bullet-}$ versus other possible ROS/RNS, we treated the probe with xanthine and xanthine oxidase, (X/XO) which is a well known biochemical assay combination that gives rise to uric acid production and also $O_2^{\bullet-}$ as a byproduct. The production of $O_2^{\bullet-}$ was verified indirectly by measuring uric acid formation at 292 nm (data not shown).[28] Theoretically, 1 mM xanthine produces 1/3 mM $O_2^{\bullet-}$ under physiological conditions.[37] **HemiSe** showed a strong "turn-on" emission centered at 439 nm upon the reaction with superoxide produced by xanthine/xanthine oxidase (X/XO) within 30 min. Superoxide dismutase (SOD) is known to convert $O_2^{\bullet-}$ radical to hydrogen peroxide (H_2O_2) or molecular oxygen (O_2) during differing catalytic steps at the same copper (Cu^{2+}) active site.[28] The fluorescence of **HemiSe** was weakened by the introduction of SOD, confirming that the "turn-on" fluorescence response of **HemiSe** was indeed superoxide-dependent (Figure 5).

Next, to demonstrate biological applications of the **HemiSe** in live cell imaging, Raw 264.7 macrophage cells were selected as a biological medium for these live cell experiments. First, we performed the cell viability assay study to confirm the biocompatibility of **HemiSe**. Raw 264.7 macrophage cells were preincubated with various concentrations of **HemiSe** (0.0, 10.0, 20.0, 30.0, 40.0 μM). MTT-1 cell proliferation assays were carried out after cells were preincubated in **HemiSe** for 3 h. The cell viability test data confirms that no substantial decrease in cell viability after treatment with **HemiSe** occurs; these results confirm that there is no significant cytotoxicity of **HemiSe** within the HeLa cells up to 40.0 μM and over a period of 3 h. These data help us gain a better understanding for potential application of **HemiSe** in live cell imaging (Fig. S14, Supporting Information).

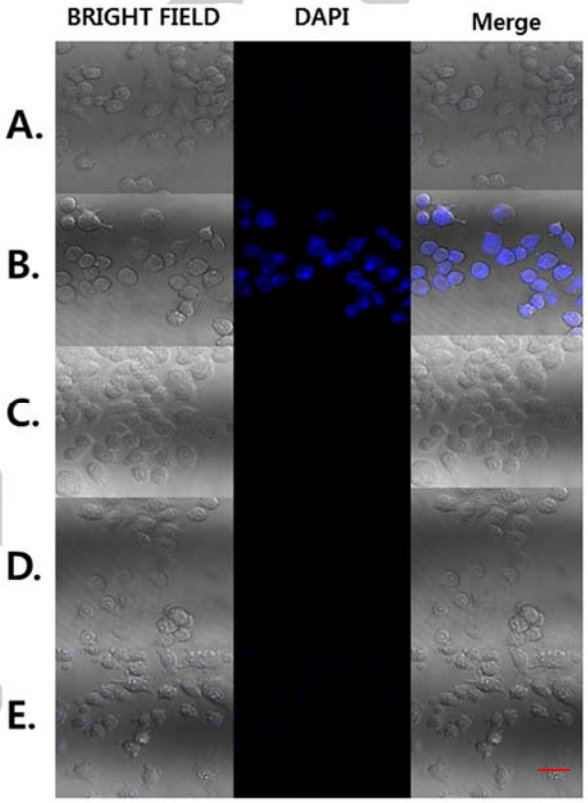

Figure 6. Confocal fluorescence images of exogenous ROS/RNS in living RAW 264.7 macrophage cells. All cells were pretreated with **HemiSe** (20 μM) for 30 min and washed two times with D-PBS; A) Control, **HemiSe** (B) $O_2^{\bullet-}$ (200 μM); C) OCl^- (200 μM); D) $ONOO^-$ (200 μM); E) H_2O_2 (200 μM) in D-PBS containing 15% of DMF, respectively. Scale bar: 10 μm.

10.1002/asia.201801339

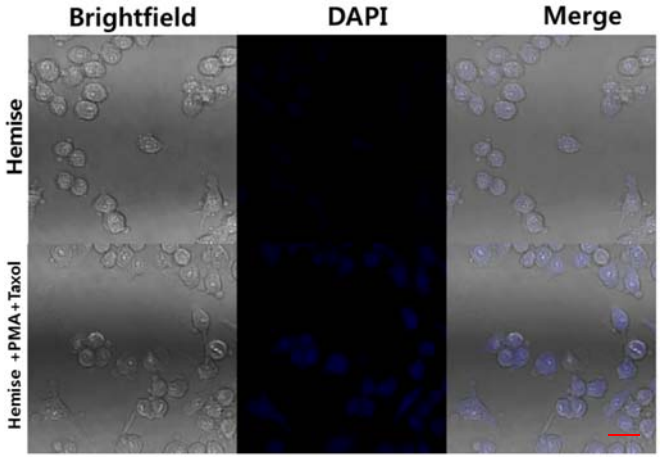

Figure 7. Confocal fluorescence images of endogenous $O_2^{\bullet-}$ with **HemiSe** in RAW 264.7 macrophages**:** non-treated cells (**HemiSe** 20 μm only); cells were pre-stimulated with PMA and taxol for 20 min within **HemiSe** (20 μM). 15% of DMF were added before imaging. Scale bar: 10 μm.

To support our results that the fluorescence response observed by the reaction only of $O_2^{\bullet-}$ and **HemiSe** by the live confocal fluorescence microscopy, macrophage cells RAW 264.7 [28] were treated with **HemiSe** for 30 min followed by incubation with 10.0 eq. of $O_2^{\bullet-}$, OCl^-, $ONOO^-$, H_2O_2 for 5 min in the presence of 15 % DMF, respectively. The confocal fluorescence images reveal a strong deep blue emission fluorescence response which appeared within RAW 264.7 macrophage cells after treatment with $O_2^{\bullet-}$; no increase in emission intensity after treatment with other ROS/RNS was observed which confirmed is it likely that **HemiSe** only undergoes reaction with $O_2^{\bullet-}$ in the living cells present in the assay and this is confirmed by testing various concentrations of $O_2^{\bullet-}$ in cell assays (Figure 6 and Fig. S19-21, Supporting Information). Then, from these results, **HemiSe** successfully demonstrated cell membrane permeability and detection of exogenous $O_2^{\bullet-}$ in live cells; therefore, this constitutes the detection molecular ions under endogenous $O_2^{\bullet-}$ in excellent model systems.

To confirm the ability of **HemiSe** for the detection of endogenous $O_2^{\bullet-}$ in live cells, RAW 264.7 macrophage cells were activated by the phorbol 12-myristate 13-acetate (PMA) to produce endogenous $O_2^{\bullet-}$.[38] Moreover, the addition of taxol together with PMA potentiated the production of $O_2^{\bullet-}$ up to 2-fold.[39] Thus, $O_2^{\bullet-}$ was generated in RAW 264.7 macrophage cells co-incubated with 1 μg/mL of PMA, 20 μM of taxol and HemiSe for 20 min at 37°C under 5% CO_2. Then, the addition of 15% of DMF in PBS was carried out 5 min before imaging. As shown in Figure 7 and relative intensity pixel data (Fig.S21, Supporting Information), this combination showed a blue fluorescence signal compound to when cells were treated with HemiSe only, which did not produce fluorescence. From these results, we have demonstrated that **HemiSe** is cell membrane permeable and the detection of $O_2^{\bullet-}$ in live cells is possible in real time manner.

Conclusions

Herein, we have developed a hemicyanine-embedded diphenylselenide (**HemiSe**)-based probe for the selective detection of superoxide radical anion. The probe shows excellent sensitivity and selectively towards superoxide and showed "turn-on" fluorescence upon addition of superoxide. The time response profile of the probes to $O_2^{\bullet-}$ by 13 minutes, and an increase in the emission intensity gave saturation value 20-fold. The detection limit of the probe is 11.9 nM. In the current system, diphenylselenide acts as a quencher; therefore, in the absence of $O_2^{\bullet-}$, the fluorescence of **HemiSe** is quenched due to the intramolecular photoinduced electron transfer (PET) process made available from the Se group, and shows negligible fluorescence and a negation in the quantum yield from what is often inherent in cyanine systems. Surprisingly, instead of undergoing reaction with selenide and forming selenoxide, $O_2^{\bullet-}$ undergoes reaction with the double-bond within **HemiSe** and forms a proposed hydroperoxide product that is capable of blocking the PET effect and affords a blue emission centered at 439 nm. The probe can also be used for the endogenous detection of $O_2^{\bullet-}$ with a "turn-on" response in the RAW264.7 cells system. This unit will be further studied in the context of versatile approaches to detection and therapeutics in neurodegenerative disease research as explored and unravelled by confocal microscope imaging in future studies.

Experimental Section

Measurements and materials

General considerations: All chemicals used herein were used as received from commercial suppliers (Aldrich, Tokyo Chemical Industry). ^1H, ^{13}C, and ^{77}Se NMR spectra were acquired using a Bruker Avance 400 and Agilent-NMR-vnmrs 600 MHz spectrometer. Tetramethylsilane and dimethyl selenide was used as external standards. ESI-mass spectrometry was performed on a BRUKER micrOTOF-QⅡ by the research support staff at KAIST. A Time-of-Flight mass spectrometer was operated at a resolution of 20,000. Absorption spectra were measured using a JASCO V–530 spectrophotometer. Fluorescence measurements were carried out with a Shimadzu RF–5301pc spectrofluorophotometer and Thermo Scientific Varioskan flash multimode reader.

DFT calculations.

The molecular structures of **HemiSe** and **HemiSe[OOH]** and their HOMO-LUMO levels were obtained using density functional theory (DFT) calculations through the use of Gaussian 09 software (B3LYP method with

6-311g* basis set for Se only and 6-31g* basis set for all other atoms). All calculations were performed with the gas phase.

Synthesis

The 2-(phenylseleno)-benzaldehyde, intermediate was synthesized according to a known literature [40].

Synthesis of **HemiSe**. To a stirred solution of(E)-1,1,3-trimethyl-2-(2-(phenylselanyl)styryl)-1H-benzo[e]indol-3-ium To a well-stirred solution of aldehyde (0.090 g, 0.343 mmol) in 10 mL of dry EtOH was added 1,1,2,3-tetramethyl-1H-benzo[e]indolium hexafluorophosphate (0.140 gm, 0.378 mmol) at room temperature. The resulting mixture was then stirred at room temperature for 15 min. The mixture was then refluxed for 12 h to yield a dark red mixture. The resulting residue was treated with aqueous HCl (1M, 1 mL), H_2O (4 mL), and EtOAc (10 mL). The mixture was warmed to room temperature and diluted with CH_2Cl_2. The mixture was washed with water, brine and dried with drying agent ($MgSO_4$), and the solvents volatiles were then evaporated. The residue was purified by silica gel column chromatography using CH_2Cl_2/MeOH (9:1) as an eluent to give **HemiSe** (0.100 g, 63 %) as a dark orange solid. IR ($CHCl_3$): υ_{max} 3424 (s), 3020 (w), 2923 (m), 1698 (w), 1652 (w), 1635 (w), 1558 (m), 1540 (m), 1396 (m), 1317 (s), 1216 (w), 840 (m), 757 (s) cm^{-1}; ^{1}H NMRS (600 MHz, CD_2Cl_2): δ 8.86 (d, J_{H-H} = 16.3 Hz, 1H), 8.26 – 8.19 (m, 2H), 8.17 (d, J_{H-H} = 8.8 Hz, 1H), 8.11 (d, J_{H-H} = 8.2 Hz, 1H), 7.85 – 7.78 (m, 2H), 7.77 (d, J_{H-H} = 9.0 Hz, 1H), 7.72 (t, J_{H-H} = 7.6 Hz, 1H), 7.67 – 7.57 (m, 2H), 7.57 – 7.49 (m, 1H), 7.47 – 7.41 (m, 1H), 7.41 – 7.35 (m, 2H), 7.32 (t, J_{H-H} = 7.6 Hz, 2H), 7.27 (d, J_{H-H} = 7.1 Hz, 1H), 4.23 (s, 3H), 1.89 (s, 6H). ^{13}C NMRS (150 MHz, $CDCl_3$): 183.1, 152.7, 138.7, 137.2, 136.3, 135.0, 134.8, 134.1, 133.9, 131.8, 131.4, 131.0, 130.3, 130.0, 129.9, 129.8, 128.8, 128.7, 127.8, 127.5, 122.9, 113.1, 112.0, 54.3, 34.8, 25.9. ^{77}Se NMRS (76.5 MHz, $CDCl_3$): 366.82. MS/EI m/z: Calculated for $C_{29}H_{26}NSe$ is 468.1230 found 468.1286.

Cell Maintenance and fluorescence imaging

The RAW264.7 cells were cultured in Dulbecoco modified eagle medium essential medium (DMEM, Gibco) supplemented with 10 % (v/v) fetal bovine serum (Gibco) and 1% penicillin/streptomycin (100 U/mL, Gibco). The RAW264.7 cells were seeded at a density of 0.5 ×10^5 cells on sterilized μ-slides (Ibidi, Munchen, Germany). After 24 h, for exogenous ROS/RNS test, 20 μM **HemiSe** were incubated for 30 min at 37 °C. Next, cells washed with D-PBS for 2 times and 200 μM of O_2^-, OCl^-, $ONOO^-$, H_2O_2 in Dulbecco's phosphate buffered saline (D-PBS, 10 mM, pH7.4) were added containing 15 % DMF, respectively. For endogenous experiment, cells were co-incubated with 1 μg/mL of PMA, 20 μM of taxol and **HemiSe** (20 μM) for 20 min at 37 °C. Approximately 5 min before imaging 15 % DMF in D-PBS was added. Fluorescent images were acquired on Zeiss LSM 780 (Carl Zeiss, Jena, Germany) laser scanning confocal microscope and a 40× and 63× objective lens was used. The excitation wavelength was 405 nm and the detection wavelength were 410–498 nm.

Acknowledgements

Prof. H. S. Park acknowledges support from by a grant from Samsung Science & Technology Foundation (SSTF-BA1702-09). The Molecular Logic Gate Laboratory operated by Prof. D. G. Churchill acknowledges support from the Mid-Career Researcher Program through the NRF (National Research Foundation) of Korea (NRF-2014R1A2A1A11052980) funded by the MEST. Tesla Yudhistira (LPDP/201412022313) acknowledges Lembaga Pengelola Dana Pendidikan (LPDP) Indonesia Endowment Fund for the fellowship and KAIST for providing research facilities. Dr. Mahesh B. Halle acknowledges the BK21plus research fellowship and KAIST for providing research facilities. The research support staff at KAIST facilitated the acquisition of MS data.

Keywords: superoxide radicals • fluorescence • live cell imaging • phenylselenide • reactive oxygen species

References

[1] M. P. Murphy, *Biochem. J.,* **2009,** *417*, 1-13.
[2] M. B. Hampton, A. J. Kettle, C. C. Winterbourn, *Blood*, **1998,** *92*, 3007-3017.
[3] S. Cemerski, A. Cantagrel, J. P. Van Meerwijk, P. Romagnoli, *J. Biol. Chem*., **2002,** *277*, 19585-19593.
[4] a) M, Valko, D. Leibfritz, J. Moncol, M. T. Cronin, M. Mazur, J. Telser, *Int. J. Biochem. Cell. Biol.,* **2007,** *39*, 44-84; S. Amor, F. Puentes, D. Baker, P. Van der Valk, *Immunology*, **2010**, *129*, 154-169; c) L. Sevenich, *Front. Immunol*., **2018**, *697*, 1-15; d) S. Mammana, P. Fagone, E. Cavalli, M. S. Basile, M. C. Petralia, F. Nicoletti, P. Bramanti, E. Mazzon, *Int. J. Mol. Sci.*, **2018**, *831*, 1-20.
[5] a) D. T. Sawyer, J. S. Valentine, *Acc. Chem. Res.*, **1981**, *14*, 393-400; b) F. Dubnikova, R. Kosloff, J. Almog, Y. Zeiri, R. Boese, H. Itzhaky, A. Alt, E. Keinan, *J. Am. Chem. Soc.*, **2005**, *127*, 1146-1159.
[6] J. F. Turrens, *J. Physiol.,* **2003,** *552*, 335-344.
[7] T. Inoue, Y. Suzuki-Karasaki, *Free Radic. Biol. Med.*, **2013,** *61*, 273-284.
[8] Y. W. Yap, M. Whiteman, N. S. Cheung, *Cell. Signal.*, **2007,** *19*, 219-228.
[9] A. A. Kelkar, J. Butler, E. B. Schelbert, S. J. Greene, A. A. Quyyumi, R. O. Bonow, I. Cohen, M. Gheorghiade, M. J. Lipinski, W. Sun, D. Luger, S. E. Epstein, *J. Am. Coll. Cardiol.*, **2015,** *66*, 2038-2047.
[10] E. A. Kaperonis, C. D. Liapis, J. D. Kakisis, D. Dimitroulis, V. G. Papavassiliou, *Eur. J. Vasc. Endovasc. Surg.,* **2006,** *31*, 386-393.
[11] S. L. Marklund, A. Bjelle, L.G. Elmqvist, *Ann Rheum. Dis.*, **1986,** *45*, 847-851.
[12] U. Asmat, K. Abad, K. Ismail, *Saudi Pharm. J.,* **2016,** *24*, 547-553.
[13] J. Q. Liu, I. N. Zelko, E. M. Erbynn, J. S. Sham, R. J. Folz, *Am. J. Physiol. Lung Cell Mol. Physiol.,* **2006,** *290*, L2-L10.
[14] K. K. Narayan, M. J. Im, P. N. Manson, *Surgical Forum*, **1985,** *36*, 593-595.
[15] C. Nathan, A. Cunningham-Bussel, *Nat. Rev. Immunol.,* **2013,** *13*, 349-361.
[16] M. P. Murphy, A. Holmgren, N. G. Larsson, B. Halliwell C. J. Chang, B. Kalyanaraman, S. G. Rhee, P. J. Thornalley, L. Partridge, D. Gems, T. Nystrom, V. Belousov, P. T. Schumacker, C. C. Winterbourn, *Cell Metab*., **2011,** *13*, 361-366.
[17] X. Zhuang, S. Liu R. Zhang F. Song, Z. Liu, S. Liu, *Anal. Chem.* **2014,** *86*, 11599-11605.
[18] F. Dondurmacoglu, A. N. Avan, R. Apak, *Anal. Methods*, **2017,** *9*, 6202-6212.
[19] B. Kalyanaraman, B. P. Dranka, M. Hardy, R. Michalski, J. Zielonka, *Biochim. Biophys. Acta,* **2014,** *1840*, 739-744.
[20] H. Flamm, J. Kieninger, A. Weltin, G. A. Urban, *Procedia Eng.,* **2015,** *120*, 26-30.
[21] M. Yamato, T. Egashira, H. Utsumi, *Free Radic. Biol. Med*., **2003,** *35*, 1619-1631.
[22] A. P. de Silva, H. Q. N. Gunaratne, T. Gunnlaugsson, A. J. M. Huxley, C. P. McCoy, J. T. Rademacher, T. E. Rice, *Chem. Rev.,* **1997,** *97*, 1515-1566.
[23] a) J. Chan, S. C. Dodani, C. J. Chang, *Nat. Chem.*, **2012,** *4*, 973-984 b) L. Kupershmidt, Z. Okun, T. Amit, S. Mandel, A. Mahammed, O. Bar-Am, Z. Gross, M. B. Youdim, *J. Neurochem.*, **2010**, *113*, 363-373..
[24] S. T. Manjare, S. Kim, W. D. Heo, D. G. Churchill, *Org. Lett.,* **2014,** *16*, 410-412.
[25] J. J. Gao, K. H. Xu, B. Tang, L. L. Yin, G. W. Yang, L. G. An, *Febs J.* **2007,** *274*, 1725-1733.
[26] J. Zielonka, B. Kalyanaraman, *Free Radic. Biol. Med*., **2010,** *48*, 983-1001.
[27] B. Kalyanaraman, B, M. Hardy, R. Podsiadly, G. Cheng, J. Zielonka, *Arc. Biochem. Biophys.,* **2017,** *617*, 38-47.

10.1002/asia.201801339

[28] J. Zhang, C. Li, R. Zhang, F. Zhang, W. Liu, X. Liu, S. M. Y Lee, H. Zhang, *Chem. Comm.* **2016,** *52*, 2679-2682.
[29] X. Li, X. Gao, W. Shi, H. Ma, *Chem. Rev.*, **2014,** *114*, 590-659.
[30] a) S. V. Mulay, M. Choi, Y. J. Jang, Y. Kim, S. Jon, D. G. Churchill *Chem. Eur. J.,* **2016,** *22*, 9642-9648; b) T. Yudhistira, S. V. Mulay, K. J. Lee, Y. Kim, H. S. Park, D. G. Churchill, *Chem. Asian J.* **2017,** *12*, 1927-1934; c) S. T. Manjare, J. Kim, Y. Lee, D. G. Churchill, *Org. Lett.*, **2014,** *16*, 520-523; d) S. V. Mulay, Y. Kim, K. J. Lee, T. Yudhistira, H. S. Park, D. G. Churchill, *New J. Chem.,* **2017**, *41*, 11934-11940.
[31] a) Y. Kim, M. Choi, S. T. Manjare, S. Jon, D. G. Churchill, *RSC Adv.* **2016,** *6*, 32013-32017; b) S. V. Mulay, T. Yudhistira, M. Choi, Y. Kim, J. Kim, Y. J. Jang, S. Jon, D. G. Churchill, *Chem. Asian J.,* **2016,** *11*, 3598-3605.
[32] a) A. P. Gorka, R. R. Nani, M. J. Schnermann, *Org. Biomol. Chem.*, **2015**, *13*, 7584-7598; b) B. Jędrzejewska, J. Kabatc, M. Pietrzak, J. Pączkowski, *Dyes Pigm.*, **2003**, *58*, 47-58.
[33] a) A. Parrot, A. Bernard, A. Jacquart, S. A. Serapian, C. Bo, E. Derat, O. Oms, A. Dolbecq, A. Proust, R. Metivier, P. Mialane, G. Izzet, *Angew. Chem.,* **2017**, *56*, 4872-4876; b) D. Moldenhauer, F. Groehn, *Chem. Eur. J.*, **2017**, *23,* 3966-3978; c) S. Deshpande, H. Kumbhar, G. Shankarling, *J. Lumin.*, 2016, 179, 314-321.
[34] a) A. V. Chernyshev, I. V. Dorogan, N. A. Voloshin, A. V. Metelitsa, V. I. Minkin, *Dyes. Pigm.* **2014**, *111*, 108-115; b) R.V. Tyurin, B. S. Lukyanov, A. V. Chernyshev, G. S. Borodkin, K. N. Khalanskii, L. V. Chepeleva, M. B. Lukyanova, *Chem. Het. Comp.*, **2014**, *50*, 734-741; c) A. Parrot, G. Izzet, L. Chamoreau, A. Proust, O. Oms, A. Dolbecq, K. Hakouk, H. Bekkachi, P. Deniard, R. Dessapt, P. Mialane, *Inorg. Chem*, **2013**, *52*, 11156-11163; d) S. M. Aldoshin, V. V. Tkachev, K. N. Khalanskii, B. S. Lukyanov, V. I. Minkin, A. N. Utenyshev, Yu. S. Alekseenko, S. O. Bezuglyi, *Russ. Chem. Bull.*, **2011**, *60*, 1380-1383.
[35] a) S. A. Samsoniya, M. V. Trapaidze, N. N. Nikoleishvili, K. G. Japaridze, J. P. Maisuradze, U. Kazmaier, *Chem. Heterocyl. Compd.*, **2011**, *47*, 1098- 1104; b) S. A. Samsoniya, M. V. Trapaidze, N. N. Nikoleishvili, K. G. Japaridze, J. P. Maisuradze, U. Kazmaier, *Chem. Heterocycl. Compd.*, **2010**, *46*, 1020-1022; c) Sh. A. Samsoniya, M. V. Trapaidze, N. N. Nikoleishvili, K. G. Japaridze, J. P. Maisuradze, U. Kazmaier, *Chem. Heterocycl. Compd.*, **2010**, *46*, 1016-1019.
[36] a) Y. Zhang, L. Guan, H. Yu, Y. Yan, L. Du, Y. Lui, M. Sun, D. Huang, S. Wang, *Anal. Chem.*, **2016**, *88*, 4426-4431; b) S. Samanta, P. Dey, A. Ramesh, G. Das, *Chem. Commun.*, **2016**, *52*, 10381-10384; c) T. Yu, G. Yin, T. Niu, P. Yin, H. Li, Y. Zhang, H. Chen, Y. Zeng, S. Yao, *Talanta,* **2018**, *176*, 1-7;d) Y. Sun, S. Fan, S. Zhang, D. Zhao, L. Duan, R. Li, *Sens. Actuators, B*, **2014**, *193*, 173-177;e) Y. Sun, D. Zhao, S. Fan, L. Duan, R. Li, *J. Agric. Food Chem.* **2014**, *62*, 3405-3409; f) X. L. Zheng, H. Li, W. Feng, H. C. Xia, Q.H. Song, *ACS. Omega*, **2018**, *3*, 1181-11837.
[37] E. E. Kelley, A. Trostchansky, H. Rubbo, B. A. Freeman, R. Radi, M. M. Tarpey, *J. Biol. Chem.*, **2004,** *279*, 37231-37234.
[38] S. Qiao, W. Li, R. Tsubouchi, M. Haneda, K. Murakami, F. Takeuchi, Y. Nisimoto, M. Yoshino, *Free Radic. Res.*, **2005**, *39*, 995-1003; J. Gieche, J. Mehlhase, A. Licht, T. Zacke, N. Sitte, T. Grune, *Biochim. Biophys. Acta,* **2001,** *1538,* 321-328.
[39] H. O. Pae, C. D. Jun, J. C. Yoo, H. J. Kwak, S. J. Lee, Y. A. Kook, R. K. Park, H. T. Chung, *Immunopharmacol. Immunotoxicol.*, **1998**, *20*, 27-37.
[40] R. Dubey, H. Lee, D. H. Nam, D. Lim, *Tetrahedron Lett.,* **2011,** *52*, 6839-6842.

10.1002/asia.201801339

WILEY-VCH

Entry for the Table of Contents

Layout 2:

FULL PAPER

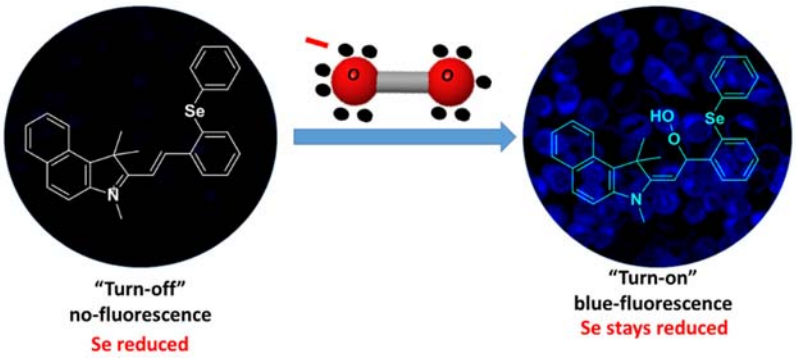

*Mahesh B. Halle, Kyung Jin Lee, Tesla Yudhistira, Jae Hyuck Choi, Hee-Sung Park, and David G. Churchill**

Page No. – Page No.

A hemicyanine-embedded diphenylselenide-containing probe "HemiSe" in which $SePh_2$ stays reduced for selective detection of superoxide in living cells.